Journal of Nuclear Medicine, published on December 18, 2020 as doi:10.2967/jnumed.120.254516

Comparative preclinical biodistribution, dosimetry and endoradiotherapy in mCRPC using $^{19}F/^{177}Lu$-rhPSMA-7.3 and ^{177}Lu-PSMA I&T

Nahid Yusufi[1], Alexander Wurzer[2], Michael Herz[1],

Calogero D'Alessandria[1], Benedikt Feuerecker[1], Wolfgang Weber[1], Hans-Jürgen Wester[2],

Stephan Nekolla[1#], Matthias Eiber[1#*]

[1]Technical University of Munich, Klinikum rechts der Isar, Department of Nuclear Medicine, Munich, Germany
[2]Chair for Pharmaceutical Radiochemistry, Technical University of Munich, Garching, Germany

joint senior authorship

First Author: Nahid Yusufi

Technical University of Munich, Klinikum rechts der Isar, Department of Nuclear Medicine

Ismaninger Straße 22, 81675 Munich, GERMANY

Email: yusufi.nahid@gmail.com

Corresponding Author: Matthias Eiber

Technical University of Munich, Klinikum rechts der Isar, Department of Nuclear Medicine

Ismaninger Straße 22, 81675 Munich, GERMANY

Email: matthias.eiber@tum.de

Running title: $^{19}F/^{177}Lu$-rhPSMA-7.3 endoradiotherapy

Keywords: PSMA; prostate cancer; ^{177}Lu-radioligand therapy; preclinical biodistribution, dosimetry

Word count: 5156

ABSTRACT

Objectives: Radiohybrid prostate-specific membrane antigen (rhPSMA)-ligands are applicable as radiochemical twins for both diagnostic PET imaging and endoradiotherapy.

Based on preliminary data as diagnostic ligand, the isomer rhPSMA-7.3 is a promising candidate for potential endoradiotherapy. The aim of this preclinical evaluation was to assess biodistribution, dosimetry and therapeutic efficacy of $^{19}F/^{177}Lu$-rhPSMA-7.3 in comparison to the established therapeutic agent ^{177}Lu-PSMA I&T (imaging & therapy).

Methods: Biodistribution of $^{19}F/^{177}Lu$-rhPSMA-7.3 and ^{177}Lu-PSMA I&T was performed in LNCaP tumor bearing SCID-mice after sacrifice at defined time points up to 7 days (n=5). Organs and tumors were dissected, injected dose per gram (%ID/g) was determined and dosimetry calculations were performed using OLINDA/EXM1.0. The therapeutic efficacy of a single dose of 30 MBq $^{19}F/^{177}Lu$-rhPSMA-7.3 (n=7) was compared with ^{177}Lu-PSMA I&T (n=7) and control groups (n=6-7) using C4-2 tumor bearing SCID-mice by evaluating tumor growth and survival over 6 weeks post treatment.

Results: The biodistribution of $^{19}F/^{177}Lu$-rhPSMA-7.3 revealed fast blood clearance (0.63 %ID/g at 1 h p.i.) and highest activity uptake in the spleen and kidneys, particularly in the first hour (33.25 %ID/g and 207.6 %ID/g, respectively at 1 h p.i.) indicating a renal excretion pathway. Compared with ^{177}Lu-PSMA I&T, $^{19}F/^{177}Lu$-rhPSMA-7.3 exhibited an initial (1 h) 2.6-fold higher tumor uptake in LNCaP xenografts and a longer retention (4.5 %ID/g vs. 0.9 %ID/g at 168 h). The tumor dose of $^{19}F/^{177}Lu$-rhPSMA-7.3 was substantially higher (e.g. 7.47 µGy/MBq vs. 1.96 µGy/MBq at 200 mm^3) compared with ^{177}Lu-PSMA I&T. In most organs absorbed doses were higher for ^{177}Lu-PSMA I&T. A single dose of $^{19}F/^{177}Lu$-rhPSMA-7.3 showed a significantly higher tumor size reduction compared with ^{177}Lu-PSMA I&T at the end of the experiment (p=0.0167). At pre-defined termination of the experiment at 6 weeks 7/7 and 3/7 mice were still alive in the

^{19}F/^{177}Lu-rhPSMA-7.3 and ^{177}Lu-PSMA I&T groups compared to the control groups with 0/7 and 0/6 mice.

Conclusions: ^{19}F/^{177}Lu-rhPSMA-7.3 can be considered a suitable candidate for clinical translation due to similar clearance kinetics and radiation dose to healthy organs, but superior tumor uptake and retention compared with ^{177}Lu-PSMA I&T. Preliminary treatment experiments showed a favorable anti-tumor response.

INTRODUCTION

In the last two decades prostate-specific membrane antigen (PSMA) targeting radiopharmaceuticals have been extensively investigated for diagnosis and treatment of prostate cancer. Several small molecule inhibitors are in different stages of clinical development. ^{68}Ga-PSMA-11 is the most widely used PSMA-ligand for diagnostics. PSMA-617 and PSMA I&T dominate the field of PSMA endoradiotherapy (*1-4*). Most recently published clinical phase II data indicate that patients with metastatic castration-resistant prostate cancer (mCRPC) for whom only limited therapeutic options are currently available, can benefit from combined PSMA targeted diagnosis and ^{177}Lu-PSMA endoradiotherapy (*5*).

Recently, the new concept of radiohybrid PSMA-ligands (rhPSMA) was introduced (*6*). These ligands are considered as fully theranostic agents due the ability to be labelled with both diagnostic and therapeutic radiometals, and ^{18}F. ^{18}F inherits several advantages for imaging, such as longer half-life, enhanced image resolution and large-scale production throughout centers using cyclotrons (*7*). Furthermore, the use of radiochemical twins (e.g. ^{18}F/^{nat}Lu-rhPSMA or ^{19}F/^{177}Lu-rhPSMA) allows pre-therapeutic PET-based imaging and dosimetry while the ^{177}Lu-labeled counterpart is used for endoradiotherapy (*8*) (Figure 1).

In first clinical retrospective reports promising results for biodistribution, image quality and tumor uptake using the ^{18}F labeled lead compound rhPSMA-7 have been reported. Additional data indicated high diagnostic performance for detection of lymph node metastases in primary prostate cancer and localization of biochemical recurrence. (*9-11*). Most recently, the different isomers (7.1, 7.2, 7.3 and 7.4) of its lead compound rhPSMA-7 have been analyzed separately in preclinical studies (Wurzer et al., in review). The single isomer rhPSMA-7.3 is regarded the most promising candidate for ^{18}F based imaging and a phase I study (NCT03995888) for assessing biodistribution and internal dosimetry in healthy individuals and in prostate cancer patients has been recently completed. Its diagnostic performance in newly diagnosed prostate cancer or suspected recurrence is investigated in two multicenter phase III studies (NCT04186819, NCT04186845).

The aim of this preclinical evaluation was to investigate the potential of $^{19}F/^{177}Lu$-rhPSMA-7.3 for PSMA-radioligand therapy by direct comparison to ^{177}Lu-PSMA I&T as established agent for clinical endoradiotherapy (*3,8,12*). We used established xenograft mice models and explored longitudinal biodistribution, dosimetry and therapeutic effect in a proof-of-concept study of both ligands.

METHODS

Mice

All animal experiments were approved by local authorities (animal license 55.2-1-54-2532-216-2015) and handled according to guidelines for the welfare and use of animals in cancer research experimentation. Male severe combined immunodeficiency (SCID CB17/Icr-Prkdc^{scid}/IcrIcoCrl) mice were used for all studies after the age of at least 6 weeks.

Cell Culture and Tumor Implantation

LNCaP and C4-2 (kind gift of G. Thalmann, University of Bern, Switzerland) cell lines were used in the tumor xenograft studies to assess tumor uptake and therapeutic effect of the assessed radioligands, respectively. C4-2 are isolated cells from a subcutaneous LNCaP xenograft tumor of a castrated mouse and reflect androgen-independent disease (*13*). The cell lines were cultivated in RPMI medium supplemented with 10 % FCS and Pen-Strep (100 IU/mL) at 37 °C in 5 % CO_2/humidified air atmosphere. For subcutaneous inoculation animals were anesthetized with 3-5 % (v/v) isoflurane inhalation and $5x10^6$ cells in 100 µL serum-free RPMI medium and 100 µL matrigel were injected in the right shoulder region.

Synthesis of $^{19}F/^{177}Lu$-rhPSMA-7.3 and ^{177}Lu-PSMA I&T

For the production of $^{19}F/^{177}Lu$-rhPSMA-7.3 1.5 GBq of carrier-added $^{177}LuCl_3$ (IDB Holland B.V.) was added to 50 nmol of the uncomplexed precursor. The solution was incubated in NaOAc (0.4 M, 400 µL, pH 5.5) and 4 mg gentisic acid at 90 °C for 30 min (radiochemical purity, RCP = 98-99%).

The synthesis of ^{177}Lu-PSMA I&T was carried out on a GRP synthesis module (Scintomics). In brief, 200 µg of the PSMA I&T precursor in 50 % (v/v) of EtOH/H_2O was labeled with 10 GBq of carrier-added $^{177}LuCl_3$ (IDB Holland B.V.) in NaOAc (0.04 M, pH 5.5) at 90 °C for 30 min with subsequent addition of 4 mg gentisic acid to prevent radiolysis (RCP = 99-100%).

Biodistribution

Approximately 40 pmol of $^{19}F/^{177}Lu$-rhPSMA-7.3 (molar activity, A_m = 30 MBq/nmol) and ^{177}Lu-PSMA I&T (A_m = 75 MBq/nmol) in 200 µL PBS were injected intravenously into the tail vein of LNCaP xenograft SCIDs for biodistribution (n = 5 per time point). The animals were sacrificed at the defined time points (1, 12, 24, 48 and 168 h p.i.). Blood and tissues of interest including tumor were collected, weighed and counted using an automated gamma counter (2480 Wizard2, PerkinElmer). Tumor-to-kidney uptake ratios were calculated, since the kidneys are one of the dose-limiting organs in clinical PSMA-directed endoradiotherapy.

Radioligand Therapy using $^{19}F/^{177}Lu$-rhPSMA-7.3 or ^{177}Lu-PSMA I&T

For endoradiotherapy studies applying $^{19}F/^{177}Lu$-rhPSMA-7.3 or ^{177}Lu-PSMA I&T, C4-2 xenograft bearing SCIDs (n = 6-7) were injected with a single dose of 30 MBq in 200 µL PBS (A_m = 30 MBq/nmol). In the respective control groups animals were injected with 1 nmol of non-radioactive rhPSMA-7.3 or PSMA I&T. PSMA expression in the xenografts were determined by pre-therapeutic PET imaging 1 h after injection of $^{18}F/^{nat}Ga$-rhPSMA-7.3 at day -3 before therapy.

Tumor size was measured once weekly by MRI until 6 weeks after injection. Tumor volumes at baseline (3 weeks after inoculation and -5 days before treatment) were not statistically different with a mean of 147.5 ± 7.3 mm^3, 122.8 ± 38.2 mm^3, 195.0 ± 41.4 mm^3 and 275.8 ± 113.6 mm^3 (p= 0.2550) for $^{19}F/^{177}Lu$-rhPSMA-7.3, rhPSMA-7.3, ^{177}Lu-PSMA I&T and PSMA I&T, respectively. Endpoint criteria were defined as tumor size exceeding 1.5 cm or critical scoring of an animal's wellbeing. Pre-defined termination of the experiment by the animal experiment license was at 6 weeks.

Magnetic Resonance Imaging

Monitoring of therapeutic effects on tumor size in xenograft animals was performed on a small animal 7 T preclinical MR-scanner (Agilent/GE magnet, Bruker AVANCE III HD electronics with ParaVision 6.0.1). Animals were anesthetized with 5 % (v/v) isoflurane inhalation and were maintained at 1.5-3 % (v/v) during scanning. T2-weighted turbo RARE images were acquired in axial orientation, with TE 40 ms, TR 3.6 s, RARE-factor 4, 4 averages, 180x180 matrix, 36x36 (mm^2) FOV, 31 slices, slice thickness 1 mm, fat saturation, receiver bandwidth 100 kHz, and total acquisition time 3 min 36 s. DICOM files from T2-weighted MR scans were analyzed in RadiAnt DICOM viewer 5.0.2. Dimensions of the ellipsoid-shaped tumors were measured based on coronar and axial images. Tumor volumes were calculated based on the formula: $V = 4/3*\pi*a*b*c$ (a/b/c= semi-axes).

Dosimetry Calculations

Five time points were used for the calculation of the time-integrated activity coefficients (TIAC). The time-integral of activity for the accumulation in the significant source organs were generated both with numerical integration and physical decay according to Yuan (*14*). Normal-organ radiation doses were estimated for the 70 kg standard adult anatomic model using time-depending organ

activity accumulation (in percent of the injected dose per gram, %ID/g) and total-body activities measured in the biodistribution studies in mice (*15,16*).

Activity accumulation in mice was converted to tissue fractional activities in the 70 kg standard adult using the relative fractional organ masses in the standard adult and the “standard” 25 g mouse. TIACs were calculated by numerical integration using the trapezoidal rule and the rest-of-body. ^{177}Lu residence times were calculated as the difference between the total-body residence time and the sum of the organ and urine residence times. Finally, the absorbed doses (in mGy/MBq) in organs of a standard adult were calculated using OLINDA/EXM1.0 according to Stabin et al. (*17*).

For estimating tumor doses the unit density sphere model described by Stabin et al. (*18*) was used. Therefore, the values for the total number of decays in MBq×h/MBq units based on the biodistribution data were inputted in OLINDA/EXM1.0.

Statistics

Data are presented as mean ± standard deviation (SD) or standard error of the mean (SEM). Mann-Whitney test was performed to compare different groups. Survival was analyzed by the Kaplan-Meyer method and Log-rank (Mantel-Cox) test. Statistical significance was considered at $p<0.05$. GraphPad Prism (version 5.04, GraphPad Software, Inc.) was used for all statistical analyses.

RESULTS

Biodistribution and Tumor Uptake of $^{19}F/^{177}Lu$-rhPSMA-7.3 and ^{177}Lu-PSMA I&T

$^{19}F/^{177}Lu$-rhPSMA-7.3 showed the typical biodistribution pattern of PSMA-targeting ligands with fast blood clearance, low uptake in normal organs, except for kidneys and spleen, and overall continuous decrease over 7 days (Figure 2A). Uptake in the kidneys and spleen was high for both ligands, with initially higher numbers for $^{19}F/^{177}Lu$-rhPSMA-7.3 (207.59 ± 30.98 %ID/g and 33.25 ± 8.62 %ID/g, respectively) compared with ^{177}Lu-PSMA I&T (165.50 ± 20.46 %ID/g and 26.06 ± 18.99 %ID/g, respectively) at 1 h (Figure 2A-B, table S1 and S2). Decline in these organs over the following days appears to be faster for $^{19}F/^{177}Lu$-rhPSMA-7.3 (35.70 ± 16.63 %ID/g in kidneys and 1.37 ± 1.21 %ID/g in spleen at 24 h) compared with ^{177}Lu-PSMA I&T (76.84 ± 22.70 %ID/g in kidneys and 4.02 ± 0.74 %ID/g in spleen at 24 h). At 168 h post-injection, only minimal activity was observed in any organ with either radiopharmaceutical.

Tumor uptake in LNCaP xenografts was 2.8-fold higher for $^{19}F/^{177}Lu$-rhPSMA-7.3 than ^{177}Lu-PSMA I&T at 1 h (12.4 ± 1.4 %ID/g vs. 4.4 ± 1.5 %ID/g) and gradually decreased for $^{19}F/^{177}Lu$-rhPSMA-7.3 until the end of study (Figure 3A and B). Tumor uptake for $^{19}F/^{177}Lu$-rhPSMA-7.3 remained higher than ^{177}Lu-PSMA I&T at all timepoints, including at 168 h post-injection where $^{19}F/^{177}Lu$-rhPSMA-7.3 showed a 4.7-fold higher activity retention (4.5 ± 1.8 %ID/g vs. 0.9 ± 0.2 %ID/g) compared with ^{177}Lu-PSMA I&T. ^{177}Lu-PSMA I&T showed a contrasting kinetic profile of tumor uptake, increasing until 24 h post-injection where upon uptake decreased for the remainder of the study. Tumor-to-kidney ratios were on average 2-fold higher in favor of $^{19}F/^{177}Lu$-rhPSMA-7.3 at all assessed timepoints (Figure 3B and Table S3).

Comparison of kinetics of retention on the logarithmic scale in kidneys, bone including marrow and tumor revealed the fastest clearance occurred in the kidneys with a similar trend towards initial higher uptake with $^{19}F/^{177}Lu$-rhPSMA-7.3 and similar clearance to ^{177}Lu-PSMA I&T (Figure 4). Clearance was slower in bone including marrow for $^{19}F/^{177}Lu$-rhPSMA-7.3. Retention was most

prolonged in tumors with a trend towards greater retention, as well as significantly higher initial uptake for $^{19}F/^{177}Lu$-rhPSMA-7.3.

Radiation Dosimetry

Absorbed doses in major organs and tissues are presented in Figure 5A and table S4/ S5. Delivered doses to all tissues were higher for ^{177}Lu-PSMA I&T compared with $^{19}F/^{177}Lu$-rhPSMA-7.3, except for the liver (1.60E-02 vs. 3.22E-03 mGy/MBq). Exemplarily, adsorbed doses in the kidney and bone marrow as the most relevant organs at risk for endoradiotherapy were 1.16 vs. 1.30 mGy/MBq and 1.05E-03 vs. 1.76E-03 mGy/MBq, for $^{19}F/^{177}Lu$-rhPSMA-7.3 vs. ^{177}Lu-PSMA I&T respectively. The differences in absorbed doses were most pronounced in the brain (3.63E-04 vs. 1.21E-03 mGy/MBq), thymus (4.85E-04 vs. 1.33E-03 mGy/MBq) and thyroid (3.92E-04 vs. 1.25E-03 mGy/MBq).

Doses delivered to the tumors are shown in Table S6 as function of the unit density sphere. $^{19}F/^{177}Lu$-rhPSMA-7.3 delivered a 2.6-fold higher radiation dose to LNCaP tumors than ^{177}Lu-PSMA I&T, independent of the tumor size (e.g. 9.90E02 vs. 3.78E02 mGy/MBq at a tumor volume of 1 mL).

Proof-of-Concept Endoradiotherapy

Changes in absolute tumor volumes and relative tumor volume changes in all groups over time are presented in Figure 6, Figure S1 and Table S7. Overall survival of all treatment groups is shown in Figure S2. Tumor growth was continuing in the control groups after application of unlabeled rhPSMA-7.3 and PSMA I&T. Median survival as determined by the endpoint tumor size >1.5 cm were 14 days for unlabeled rhPSMA-7.3 and 10.5 days for PSMA I&T.

Both tumors treated with $^{19}F/^{177}Lu$-rhPSMA-7.3 or ^{177}Lu-PSMA I&T showed growth retention. However, tumors in the ^{177}Lu-PSMA I&T group showed earlier regrowth after initial retention compared with the $^{19}F/^{177}Lu$-rhPSMA-7.3 group. By the end of the study (week 6), tumors treated

with $^{19}F/^{177}Lu$-rhPSMA-7.3 were significantly smaller than those treated with ^{177}Lu-PSMA I&T (abs. volumes: 170.3 ± 46.1 mm^3 vs. 712.2 ± 119.4 mm^3 or relative change: 1.2 ± 0.3 vs. 6.2 ± 2.7, p=0.0167). Median survival of ^{177}Lu-PSMA I&T treated animals was 35 days, while all mice treated with $^{19}F/^{177}Lu$-rhPSMA-7.3 had prolonged survival up to the end of the treatment study (week 6).

DISCUSSION

The aim of these preclinical studies was to investigate the pharmacokinetics, dosimetry and therapeutic efficacy of the novel theranostic agent $^{19}F/^{177}Lu$-rhPSMA-7.3 in comparison to the clinically established agent, ^{177}Lu-PSMA I&T. The biodistribution pattern of ^{177}Lu-PSMA I&T, was consistent with previously published preclinical data (*19,20*). A similar uptake profile in healthy organs was found for $^{19}F/^{177}Lu$-rhPSMA-7.3 over the assessment period of 7 days. However, $^{19}F/^{177}Lu$-rhPSMA-7.3 seem to have a faster binding and similar clearance kinetic than healthy tissues, demonstrated by higher values in organs, the low blood concentration in the first hours and subsequent similar decline in most organs. In contrast, while a higher amount of ^{177}Lu-PSMA I&T is present in the blood in the first hours, uptake peaks and clearance in most healthy organs are delayed. The preclinical biodistribution for $^{19}F/^{177}Lu$-rhPSMA-7.3 assessed in this study is similar to clinical data in prostate cancer patients using the F-18 labeled mixed diasteroisomeric compound rhPSMA-7 (*9*).

Our data indicate clear differences in tumor uptake between $^{19}F/^{177}Lu$-rhPSMA-7.3 and ^{177}Lu-PSMA I&T in LNCaP xenografts. In our study, $^{19}F/^{177}Lu$-rhPSMA-7.3 has a substantially higher tumor uptake compared with ^{177}Lu-PSMA I&T at all assessed timepoints up to 7 days. This corresponds with recently performed *in vitro* evaluations by Wurzer et al. of rhPSMA-7 chelated with Ga-68 (*6*). The extent of internalization in LNCaP cells of ^{68}Ga-rhPSMA-7 is considerably higher (approx. 125% of reference) than in previously assessed rates for PSMA I&T chelated with either ^{68}Ga or ^{177}Lu (range 59–76 % of reference) (*21*). In further *in vitro* characterization studies of the individual isomers of the rhPSMA-7 lead compound, rhPSMA-7.3 is characterized by a significantly higher internalization rate in LNCaP tumor cells (161.9 % of reference; Wurzer et al., in review). Wurzer et al. also reported improved binding affinities (IC_{50}) for the rhPSMA-7 isomers compared to KuE-based PSMA inhibitors, of which PSMA I&T is one (*6*).

Given their similar uptake in kidneys, the increased accumulation rate of $^{19}F/^{177}Lu$-rhPSMA-7.3 in tumor tissue resulted in improved tumor-to-kidney ratios at all assessed timepoints up to 7 days in comparison with ^{177}Lu-PSMA I&T. This preclinical observation, if preserved in clinical translation, could be a potential advantage of $^{19}F/^{177}Lu$-rhPSMA-7.3 vs. ^{177}Lu-PSMA I&T. Renal toxicity is one of the major concerns in clinical use of PSMA endoradiotherapy (*22,23*), although only rare cases of renal toxicity for PSMA endoradiotherapy are currently reported, clinical dosimetry of ^{177}Lu-PSMA-617 and ^{177}Lu-PSMA I&T indicate that a critical dose to the kidneys is reached after 4-6 cycles. Renal toxicity after radionuclide therapy is often a long-term side effect so this is especially relevant for potential future application of PSMA endoradiotherapy in earlier stages of disease progression.

Another potential at risk organ, bone marrow, also revealed similar absorbed doses with both radiopharmaceuticals. Bone marrow toxicity grade 3/4 is reported in up to one third of patients, especially in patients with diffuse bone marrow involvement (*24,25*). Yet bone marrow toxicity in patients with low bone tumor burden is rare. In summary, improved uptake in tumors at similar uptake in kidneys and bone marrow could be an indication that lower radioactive doses of $^{19}F/^{177}Lu$-rhPSMA-7.3 might be administered to achieve similar treatment effects compared with established PSMA-targeting peptides, but while allowing for more therapy sessions given the lower dose to organs-at-risk per cycle. Notably, salivary gland toxicity is a major concern using alpha-emitter and beta-emitter (*26,27*). In our preclinical study salivary gland uptake was not assessed given the differences in PSMA expression between murine and human salivary glands (*28-31*). This issue has to be either investigated within a phase I clinical trial or using different clinical models (e.g. pigs) as previously published for ^{177}Lu-PSMA 617 (*31*).

Calculations of estimated doses delivered to major human organs and tissues were performed based on the biodistribution data of $^{19}F/^{177}Lu$-rhPSMA-7.3 and ^{177}Lu-PSMA I&T over 7 days and

revealed smaller absorbed doses for $^{19}F/^{177}Lu$-rhPSMA-7.3. Dose calculations using preclinical data for ^{177}Lu-PSMA I&T have been already performed by Weineisen et al. resulting in similar absorbed doses in major organs (*32*). Clinical dosimetry data has been collected both for ^{177}Lu-PSMA I&T and ^{177}Lu-PSMA-617. Absorbed doses in organs show no substantial difference between both ligands especially for the known dose limiting organs kidneys and salivary glands (*33-38*).

A direct comparison to ^{177}Lu-PSMA-617, which is currently being evaluated in a phase III multicenter trial, was not performed in our study. However, Kuo et al. has evaluated ^{177}Lu-PSMA-617 in the same xenograft animal model the uptake in LNCaP tumor tissue and calculated the corresponding delivered dose. At all tumor volumes ^{177}Lu-PSMA-617 delivers smaller doses comparable to the values calculated for ^{177}Lu-PSMA I&T in our study (*39*). Despite differences in methodology this provides some evidence that $^{19}F/^{177}Lu$-rhPSMA-7.3 might also offer enhanced tumor-to-organ characteristics compared with ^{177}Lu-PSMA-617.

In the proof-of concept therapy study we observed a significantly higher anti-tumor effect using $^{19}F/^{177}Lu$-rhPSMA-7.3 compared with ^{177}Lu-PSMA I&T. By the end of the observation time (week 6) all tumors treated with ^{177}Lu-PSMA I&T group were exhibiting clear regrowth compared to $^{19}F/^{177}Lu$-rhPSMA-7.3, for which tumors remained a similar size compared to baseline. The substantial growth of large tumors in the control groups and in the ^{177}Lu-PSMA I&T group led to experimental termination for these mice. Thus, a clear trend to longer median survival was present for $^{19}F/^{177}Lu$-rhPSMA-7.3. When combining data from biodistribution and treatment experiments, it can be assumed that improved uptake (%ID/g) and retention subsequently leading to higher tumor doses of $^{19}F/^{177}Lu$-rhPSMA-7.3 in tumor tissue has resulted in this prolonged growth inhibition in the C4-2 xenografts.

There are limitations in our study. First, due to logistical reasons, the baseline tumor size was measured 5 days prior to treatment in all agent groups leading to an overestimation of tumor growth during the therapy phase. Between baseline measurement and the next measurements at day 1/2 tumors sizes doubled in average, so taking day 0 as reference day tumor fold-changes would be theoretically smaller in all groups. Second, the pre-defined endpoint of the study at 6 weeks is a bias for the comparison of survival between both groups. Third, the extrapolation of preclinical data in mice to potential clinical application is difficult. Reasons include differences in PSMA homologs and expression between humans and mice, non-specific uptake and in pharmacokinetics. Therefore, extrapolation of dosimetry from mice to men is prone to several potential errors. Similar to data in the literature, our preclinical dosimetry results are lower than data reported for dosimetry conducted following clinical use. However, the main message derived from our data rely on the comparison of the two ligands in an identical preclinical setting. Whether the differences observed in mice translate into clinical data needs to be investigated.

CONCLUSIONS

Our preclinical data demonstrate that $^{19}F/^{177}Lu$-rhPSMA-7.3 has broadly similar biodistribution and clearance kinetics to ^{177}Lu-PSMA I&T. However, effective doses to xenografts were substantially higher compared with ^{177}Lu-PSMA I&T at equivalent doses to normal organs. This translated into a higher anti-tumor effect in a preliminary endoradiotherapy study designating $^{19}F/^{177}Lu$-rhPSMA-7.3 as an interesting candidate for clinical translation. However, future clinical trials evaluating $^{19}F/^{177}Lu$-rhPSMA-7.3 need to investigate whether the favorable preclinical profile translates into enhanced clinical anti-tumor effect without additional safety concerns.

ACKNOWLEDGEMENTS

We thank Sybille Reder, Markus Mittelhäuser, Sandra Sühnel, Hannes Rolbieski, Birgit Blechert and Martin Grashei for technical support in the studies.

DISCLOSURE

Patent application for rhPSMA (HJW, AW and ME). HJW and ME received funding from the SFB 824 (DFG Sonderforschungsbereich 824, Project B11) from the Deutsche Forschungsgemeinschaft, Bonn, Germany and Blue Earth Diagnostics Ltd (licensee for rhPSMA) as part of an academic collaboration. HJW is founder, shareholder and advisor board member of Scintomics GmbH, Fuerstenfeldbruck, Germany. ME and WW are consultants for Blue Earth Diagnostics Ltd. No other potential conflicts of interest relevant to this article exist.

KEY POINTS

Question: Are the biodistribution, dosimetry and therapeutic efficacy comparable between ^{19}F/^{177}Lu-rhPSMA-7.3 and ^{177}Lu-PSMA I&T?

Pertinent Findings: In preclinical prostate cancer xenograft models uptake of ^{19}F/^{177}Lu-rhPSMA-7.3 was initially mainly higher with a faster clearance profile resulting in lower absorbed doses compared with ^{177}Lu-PSMA I&T. ^{19}F/^{177}Lu-rhPSMA-7.3 showed higher tumor uptake and significantly better therapeutic efficacy.

Implications for Patient Care: Preclinical data indicate a better profile for ^{19}F/^{177}Lu-rhPSMA-7.3 for radioligand treatment, which has to be explored in prospective clinical studies.

REFERENCES

1. von Eyben FE, Picchio M, von Eyben R, Rhee H, Bauman G. (68)Ga-labeled prostate-specific membrane antigen ligand positron emission tomography/computed tomography for prostate cancer: A systematic review and meta-analysis. *Eur Urol Focus*. 2018;4:686-93.
2. Perera M, Papa N, Roberts M et al. Gallium-68 prostate-specific membrane antigen positron emission tomography in advanced prostate cancer-updated diagnostic utility, sensitivity, specificity, and distribution of prostate-specific membrane antigen-avid lesions: A systematic review and meta-analysis. *Eur Urol*. 2020;77:403-17.
3. Heck MM, Tauber R, Schwaiger S et al. Treatment outcome, toxicity, and predictive factors for radioligand therapy with (177)Lu-PSMA-I&T in metastatic castration-resistant prostate cancer. *Eur Urol*. 2019;75:920-6.
4. Rahbar K, Ahmadzadehfar H, Kratochwil et al. German multicenter study investigating 177Lu-PSMA-617 radioligand therapy in advanced prostate cancer patients. *J Nucl Med*. 2017;58:85-90.
5. Seifert R, Seitzer K, Herrmann K et al. Analysis of PSMA expression and outcome in patients with advanced prostate cancer receiving (177)Lu-PSMA-617 radioligand therapy. *Theranostics*. 2020;10:7812-20.
6. Wurzer A, Di Carlo D, Schmidt A et al. Radiohybrid ligands: a novel tracer concept exemplified by (18)F- or (68)Ga-labeled rhPSMA inhibitors. *J Nucl Med*. 2020;61:735-42.
7. Sanchez-Crespo A. Comparison of Gallium-68 and Fluorine-18 imaging characteristics in positron emission tomography. *Appl Radiat Isot.* 2013;76:55-62.
8. Wester HJ, Schottelius M. PSMA-targeted radiopharmaceuticals for imaging and therapy. *Semin Nucl Med*. 2019;49:302-12.
9. Oh SW, Wurzer A, Teoh EJ et al. Quantitative and qualitative analyses of biodistribution and PET image quality of a novel radiohybrid PSMA, (18)F-rhPSMA-7, in patients with prostate cancer. *J Nucl Med*. 2020;61:702-9.
10. Eiber M, Kroenke M, Wurzer A et al. (18)F-rhPSMA-7 PET for the detection of biochemical recurrence of prostate cancer after radical prostatectomy. *J Nucl Med*. 2020;61:696-701.
11. Kroenke M, Wurzer A, Schwamborn K et al. Histologically confirmed diagnostic efficacy of (18)F-rhPSMA-7 PET for N-Staging of patients with primary high-risk prostate cancer. *J Nucl Med*. 2020;61:710-5.
12. Baum RP, Kulkarni HR, Schuchardt C et al. Lutetium-177 PSMA radioligand therapy of metastatic castration-resistant prostate cancer: Safety and efficacy. *J Nucl Med*. 2016;57:1006-13.

13. Cunningham D, You Z. In vitro and in vivo model systems used in prostate cancer research. J Biol Methods. 2015;2:e17.

14. Yuan J. Estimation of variance for AUC in animal studies. *J Pharm Sci.* 1993;82:761-3.

15. Kirschner AS, Ice RD, Beierwaltes WH. Radiation dosimetry of 131I-19-Iodocholesterol. *J Nucl Med*. 1973;14:713-7.

16. Kirschner A IR, Beierwaltes W. Letters to the editor. *J Nucl Med.* 1975. p. 248–9.

17. Stabin MG, Sparks RB, Crowe E. OLINDA/EXM: The second-generation personal computer software for internal dose assessment in nuclear medicine. *J Nucl Med*. 2005;46:1023-7.

18. Stabin MG, Konijnenberg MW. Re-evaluation of absorbed fractions for photons and electrons in spheres of various sizes. *J Nucl Med*. 2000;41:149-60.

19. Weineisen M, Schottelius M, Simecek J et al. 68Ga- and 177Lu-labeled PSMA I&T: optimization of a PSMA-targeted theranostic concept and first proof-of-concept human studies. *J Nucl Med*. 2015;56:1169-76.

20. Chatalic KLS, Heskamp S, Konijnenberg M et al. Towards personalized treatment of prostate cancer: PSMA I&T, a promising prostate-specific membrane antigen-targeted theranostic agent. *Theranostics*. 2016;6:849-61.

21. Schottelius M, Wirtz M, Eiber M, Maurer T, Wester HJ. [(111)In]PSMA-I&T: expanding the spectrum of PSMA-I&T applications towards SPECT and radioguided surgery. *EJNMMI Res*. 2015;5:68.

22. Kratochwil C, Bruchertseifer F, Rathke H et al. Targeted alpha-therapy of metastatic castration-resistant prostate cancer with (225)Ac-PSMA-617: swimmer-plot analysis suggests efficacy regarding duration of tumor control. *J Nucl Med*. 2018;59:795-802.

23. Langbein T, Chausse G, Baum RP. Salivary gland toxicity of PSMA radioligand therapy: relevance and preventive strategies. *J Nucl Med*. 2018;59:1172-3.

24. Gafita A, Fendler WP, Hui W et al. Efficacy and safety of 177Lu-labeled prostate-specific membrane antigen radionuclide treatment in patients with diffuse bone marrow involvement: a multicenter retrospective study. *Eur Urol*. 2020 Aug;78(2):148-154.

25. Hofman MS, Violet J, Hicks RJ et al. [(177)Lu]-PSMA-617 radionuclide treatment in patients with metastatic castration-resistant prostate cancer (LuPSMA trial): a single-centre, single-arm, phase 2 study. *Lancet Oncol*. 2018;19:825-33.

26. Kratochwil C, Bruchertseifer F, Rathke H et al. Targeted α-therapy of metastatic castration-resistant prostate cancer with (225)Ac-PSMA-617: swimmer-plot analysis suggests efficacy regarding duration of tumor control. *J Nucl Med*. 2018;59:795-802.

27. Rathke H, Kratochwil C, Hohenberger R et al. Initial clinical experience performing sialendoscopy for salivary gland protection in patients undergoing (225)Ac-PSMA-617 RLT. *Eur J Nucl Med Mol Imaging.* 2019;46:139-47.
28. Schmittgen TD, Zakrajsek BA, Hill RE et al. Expression pattern of mouse homolog of prostate-specific membrane antigen (FOLH1) in the transgenic adenocarcinoma of the mouse prostate model. *Prostate*. 2003;55:308-16.
29. Simons BW, Turtle NF, Ulmert DH, Abou DS, Thorek DLJ. PSMA expression in the Hi-Myc model; extended utility of a representative model of prostate adenocarcinoma for biological insight and as a drug discovery tool. *Prostate*. 2019;79:678-85.
30. Rupp NJ, Umbricht CA, Pizzuto DA et al. First clinicopathologic evidence of a non-PSMA-related uptake mechanism for (68)Ga-PSMA-11 in salivary glands. *J Nucl Med* 2019;60:1270-6.
31. Tonnesmann R, Meyer PT, Eder M, Baranski AC. [(177)Lu]Lu-PSMA-617 Salivary gland uptake characterized by quantitative in vitro autoradiography. *Pharmaceuticals*. 2019;12.
32. Weineisen M, Schottelius M, Simecek J et al. 68Ga- and 177Lu-labeled PSMA I&T: optimization of a PSMA-targeted theranostic concept and first proof-of-concept human studies. *J Nucl Med*. 2015;56:1169-76.
33. Fendler WP, Reinhardt S, Ilhan H et al. Preliminary experience with dosimetry, response and patient reported outcome after 177Lu-PSMA-617 therapy for metastatic castration-resistant prostate cancer. *Oncotarget.* 2017;8:3581-3590.
34. Delker A, Fendler WP, Kratochwil C et al. Dosimetry for 177Lu-DKFZ-PSMA-617: a new radiopharmaceutical for the treatment of metastatic prostate cancer. *Eur J Nucl Med Mol Imaging.* 2016;43:42-51.
35. Kabasakal L, Toklu T, Yeyin N et al. Lu-177-PSMA-617 prostate-specific membrane antigen inhibitor therapy in patients with castration-resistant prostate cancer: stability, bio-distribution and dosimetry. *Mol Imaging Radionucl Ther*. 2017;26:62-8.
36. Scarpa L, Buxbaum S, Kendler D et al. The 68Ga/177Lu theragnostic concept in PSMA targeting of castration-resistant prostate cancer: correlation of SUVmax values and absorbed dose estimates. *Eur J Nucl Med Mol Imaging.* 2017;44(5):788-800.
37. Violet J, Jackson P, Ferdinandus J et al. Dosimetry of 177Lu-PSMA-617 in metastatic castration-resistant prostate cancer: correlations between pretherapeutic imaging and whole-body tumor dosimetry with treatment outcomes. *J Nucl Med*. 2019;60(4):517-23.
38. Okamoto S, Thieme A, Allmann J et al. Radiation dosimetry for 177Lu-PSMA I&T in metastatic castration-resistant prostate cancer: absorbed dose in normal organs and tumor lesions. *J Nucl Med*. 2017;58:445-50.

39. Kuo H-T, Merkens H, Zhang Z et al. Enhancing treatment efficacy of 177Lu-PSMA-617 with the conjugation of an albumin-binding motif: preclinical dosimetry and endoradiotherapy studies. *Mol Pharm*. 2018;15:5183-91.

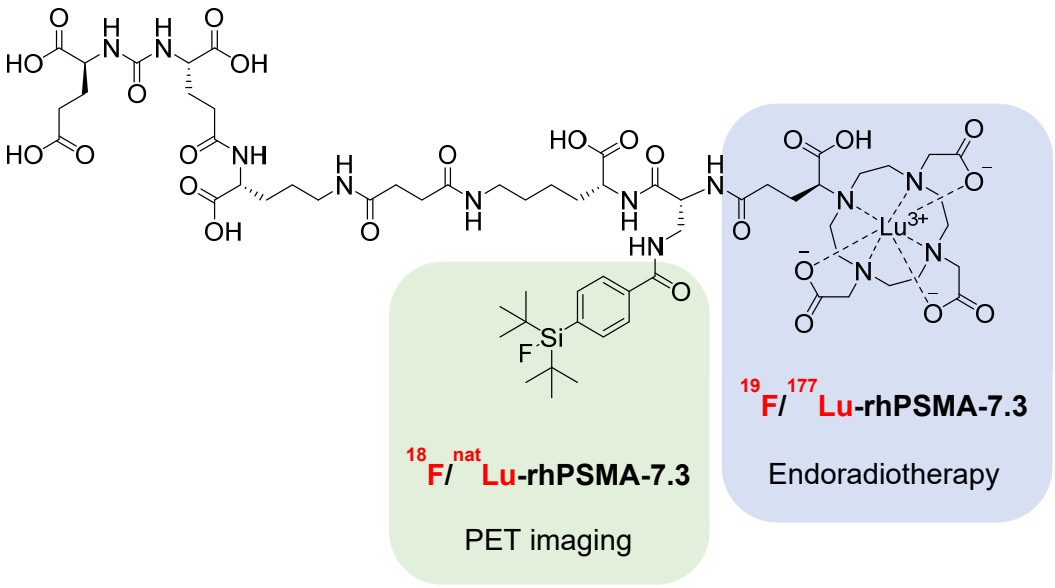

Figure 1. Radiohybrid concept of the radiochemical twins ^{18}F/^{nat}Lu-rhPSMA-7.3 and ^{19}F/^{177}Lu-rhPSMA-7.3. ^{18}F labeling at the SiFA binding site (green), while ^{nat}Lu is chelated, allows PET-based imaging. rhPSMA-7.3 chelated with ^{177}Lu (blue) and binding of nonradioactive ^{19}F is used for endoradiotherapy.

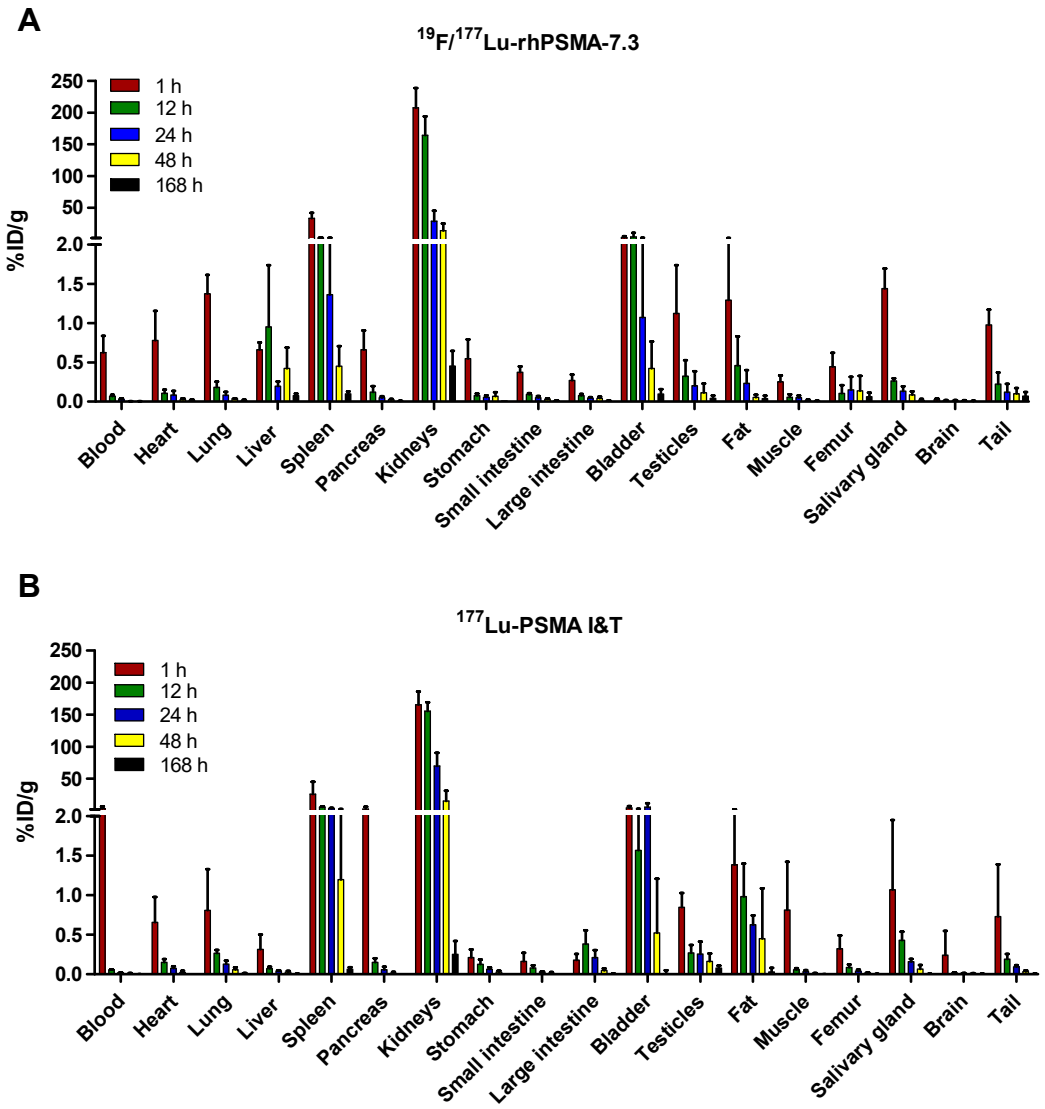

Figure 2. Biodistribution of $^{19}F/^{177}Lu$-rhPSMA-7.3 (A) and ^{177}Lu-PSMA I&T (B) at 1, 12, 24, 48 and 168 h after intravenous administration of 40 pmol of respective radio-peptide. Mean %ID/g ± SD are shown (n=5).

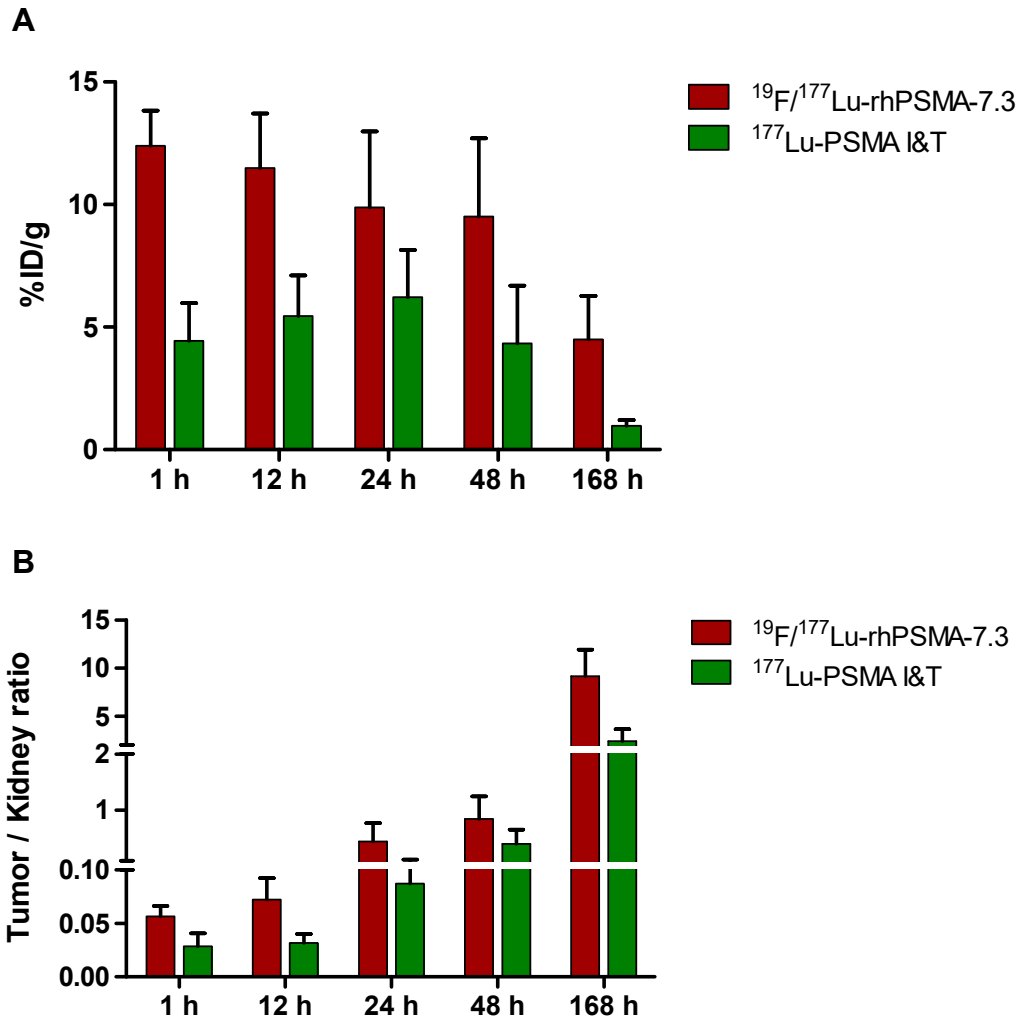

Figure 3. Activity uptake in %ID/g of $^{19}F/^{177}Lu$-rhPSMA-7.3 and ^{177}Lu-PSMA I&T in LNCaP tumors over 1 h to 168 h (A). Tumor-to-kidney uptake ratios of $^{19}F/^{177}Lu$-rhPSMA-7.3 and ^{177}Lu-PSMA I&T in the different time groups from 1 h to 168 h (B). Data are shown as mean ± SD (n=5).

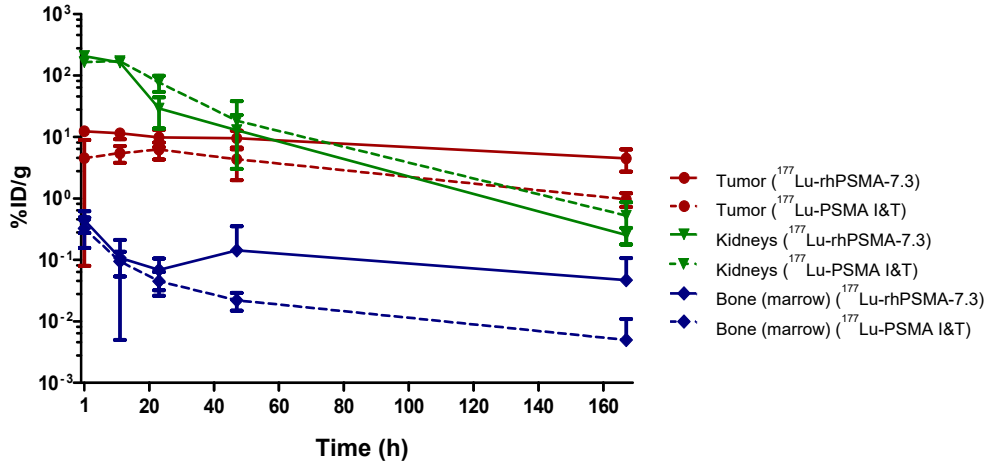

Figure 4. Plot of activity accumulation in %ID/g over time (1 to 168 h) in tumors (LNCaP), kidneys and bone (marrow) after administration of $^{19}F/^{177}Lu$-rhPSMA-7.3 (solid lines) and ^{177}Lu-PSMA I&T (dashed lines). Data are presented as mean ± SD. Clearance rates (in 1/h) for $^{19}F/^{177}Lu$-rhPSMA-7.3 and ^{177}Lu-PSMA I&T are 0.006 vs. 0.012 (tumor), 0.031 vs. 0.035 (kidneys) and 0.006 vs. 0.017 (bone/ marrow), respectively.

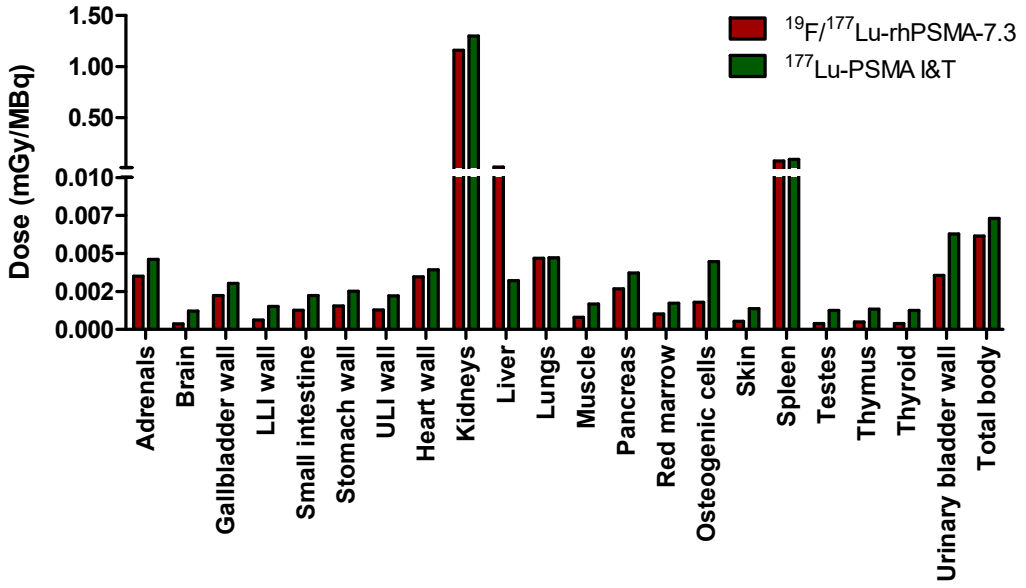

Figure 5. Calculated doses in mGy/MBq delivered to human organs and tissues for $^{19}F/^{177}Lu$-rhPSMA-7.3 and ^{177}Lu-PSMA I&T.

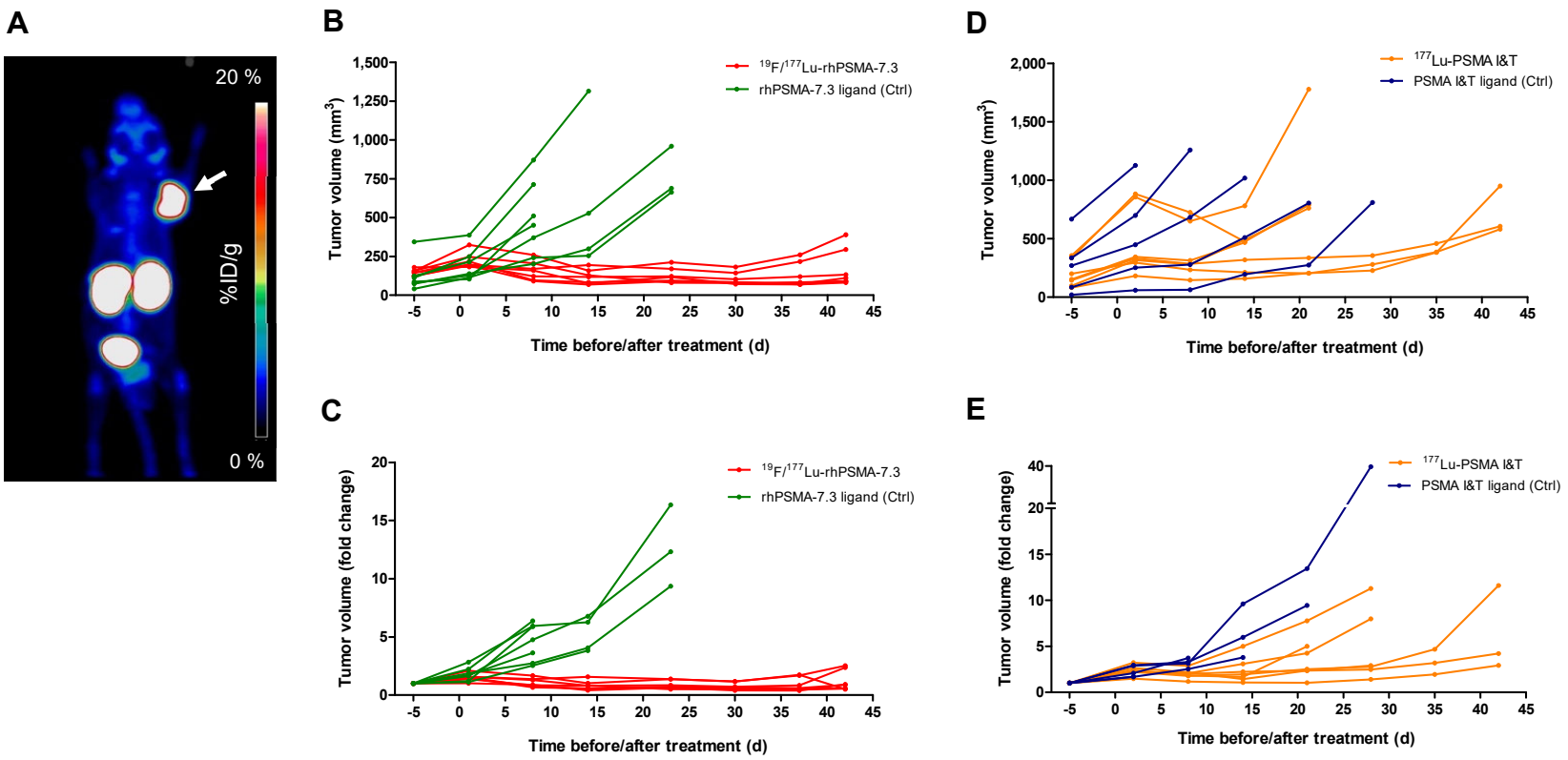

Figure 6. Representative pre-therapeutic PET image using $^{18}F/^{nat}Ga$-rhPSMA-7.3. C4-2 xenograft is indicated by the white arrow (A). Tumor growth curves of individual mice in the respective treatment and control groups of the endoradiotherapy study at days before/after treatment (day 0) are shown (B-E). In the $^{19}F/^{177}Lu$-rhPSMA-7.3/ rhPSMA-7.3 groups absolute volumes are expressed in mm^3 (B) and relative tumor volumes are given as fold-change (C). In the ^{177}Lu-PSMA I&T/ PSMA I&T groups absolute volumes are expressed in mm^3 (D) and relative tumor volumes are given as fold-change (E).

GRAPHICAL ABSTRACT

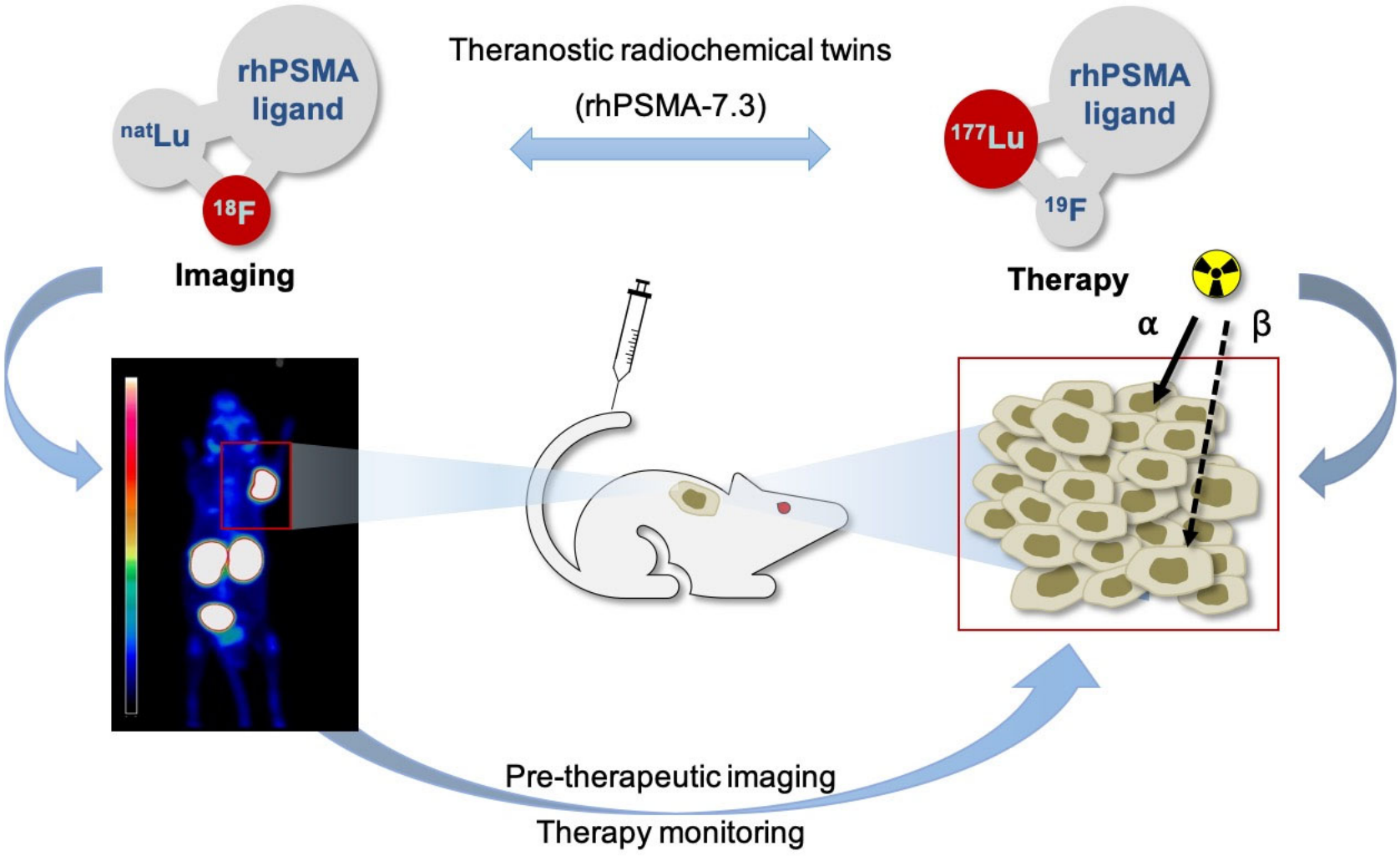

SUPPLEMENTARY MATERIAL

A

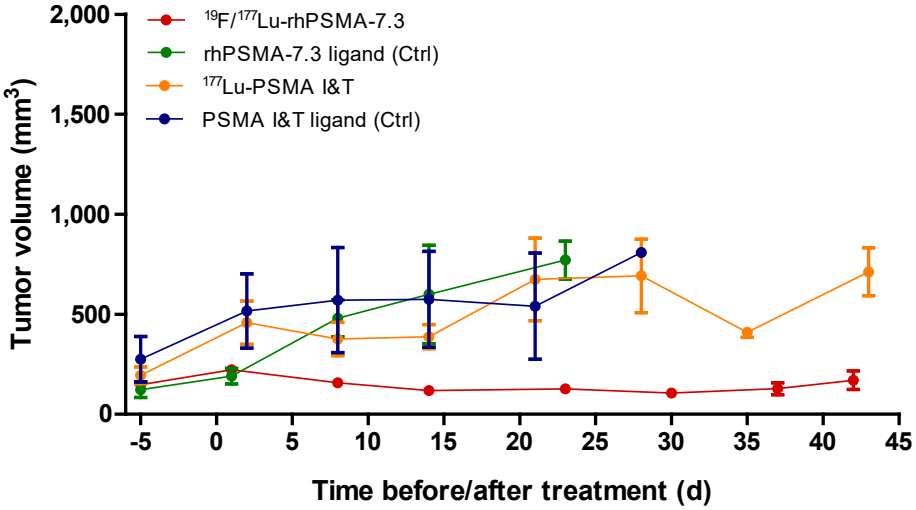

B

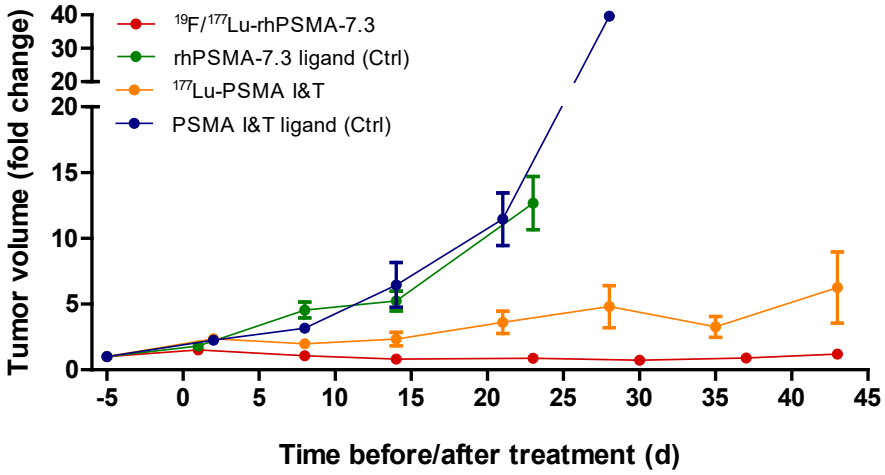

Figure S1. Tumor growth curves of the respective treatment and control groups in the ^{19}F/^{177}Lu-rhPSMA-7.3 and ^{177}Lu-PSMA I&T endoradiotherapy study at days before/after treatment (day 0). Absolute volumes in mm^3 are expressed as mean ± SEM (A) and relative tumor volumes are given as fold-change mean ± SEM (B).

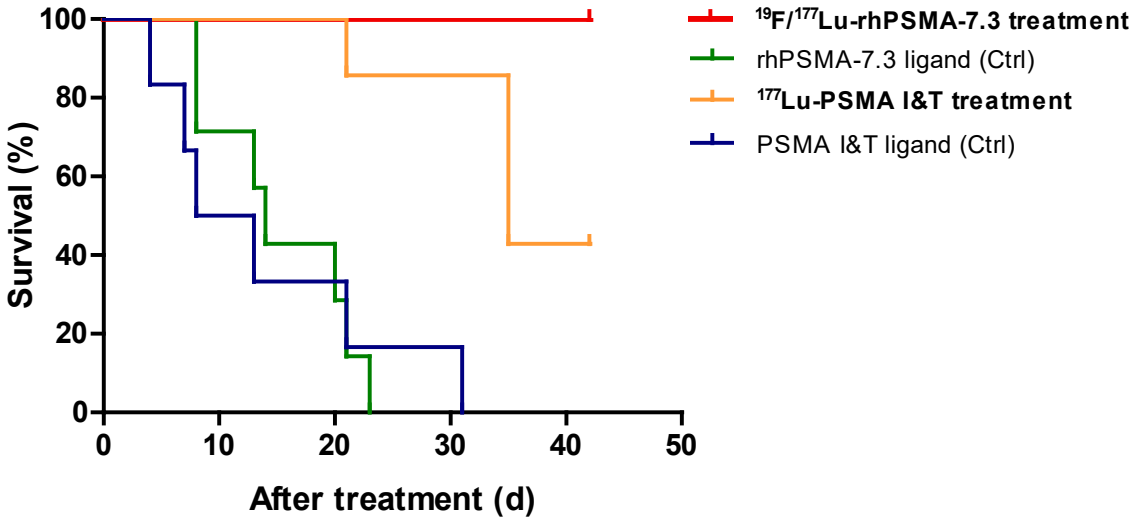

Figure S2. Kaplan-Meyer plot for survival of the treatment and control groups in the $^{19}F/^{177}Lu$-rhPSMA-7.3 and ^{177}Lu-PSMA I&T endoradiotherapy study.

Table S1. Biodistribution of $^{19}F/^{177}Lu$-rhPSMA-7.3 at 1, 12, 24, 48 and 168 h after intravenous administration. Mean and SD of %ID/g and %ID are shown (n=5).

%ID/g	1 h		12 h		24 h		48 h		168 h	
	Mean	SD	Mean	SD	Mean	SD	Mean	SD	Mean	SD
Blood	0.63	0.21	0.07	0.02	0.03	0.01	0.01	0.00	0.00	0.01
Heart	0.78	0.37	0.11	0.04	0.08	0.05	0.03	0.02	0.02	0.01
Lung	1.37	0.24	0.18	0.07	0.08	0.04	0.04	0.01	0.02	0.01
Liver	0.66	0.09	0.95	0.79	0.20	0.06	0.43	0.26	0.09	0.02
Spleen	33.25	8.62	2.57	0.72	1.37	1.21	0.50	0.35	0.12	0.03
Pancreas	0.66	0.25	0.12	0.08	0.05	0.02	0.03	0.01	0.01	0.00
Kidneys	207.59	30.98	164.25	29.64	35.70	16.63	14.43	10.95	0.48	0.14
Stomach	0.55	0.24	0.08	0.02	0.06	0.02	0.07	0.05	0.01	0.00
Small intestine	0.38	0.07	0.09	0.02	0.05	0.02	0.04	0.01	0.01	0.00
Large intestine	0.27	0.07	0.08	0.02	0.04	0.01	0.04	0.02	0.01	0.00
Bladder	2.86	2.22	4.00	6.32	1.07	1.42	0.45	0.35	0.10	0.06
Testicles	1.12	0.62	0.33	0.20	0.21	0.18	0.12	0.12	0.05	0.03
Fat	1.29	1.00	0.46	0.37	0.23	0.17	0.06	0.04	0.04	0.04
Muscle	0.26	0.08	0.06	0.04	0.05	0.02	0.02	0.01	0.01	0.00
Bone	0.45	0.17	0.11	0.10	0.15	0.17	0.16	0.25	0.09	0.12
Salivary gland	1.44	0.25	0.27	0.03	0.13	0.06	0.09	0.04	0.03	0.01
Brain	0.03	0.01	0.01	0.00	0.02	0.00	0.01	0.01	0.01	0.00
Tail	0.98	0.19	0.22	0.15	0.12	0.11	0.11	0.10	0.10	0.11
%ID	**1 h**		**12 h**		**24 h**		**48 h**		**168 h**	
	Mean	SD	Mean	SD	Mean	SD	Mean	SD	Mean	SD
Blood	0.30	0.15	0.03	0.01	0.01	0.01	0.00	0.00	0.00	0.00
Heart	0.09	0.05	0.01	0.00	0.01	0.00	0.00	0.00	0.00	0.00
Lung	0.21	0.06	0.03	0.01	0.01	0.01	0.01	0.00	0.00	0.00
Liver	0.55	0.10	0.64	0.51	0.15	0.04	0.31	0.18	0.07	0.02
Spleen	0.81	0.08	0.05	0.01	0.03	0.01	0.01	0.00	0.00	0.00
Pancreas	0.09	0.03	0.01	0.01	0.01	0.00	0.00	0.00	0.00	0.00
Kidneys	62.43	7.60	42.69	4.50	15.72	14.19	3.87	2.57	0.13	0.03
Stomach	0.08	0.04	0.01	0.00	0.01	0.00	0.01	0.00	0.00	0.00
Small intestine	0.18	0.04	0.05	0.01	0.03	0.02	0.02	0.01	0.01	0.00
Large intestine	0.08	0.03	0.02	0.01	0.01	0.00	0.01	0.01	0.00	0.00
Bladder	0.07	0.06	0.08	0.15	0.02	0.02	0.01	0.01	0.00	0.00
Testicles	0.23	0.15	0.06	0.04	0.04	0.04	0.02	0.02	0.01	0.01
Fat	0.06	0.05	0.01	0.01	0.01	0.02	0.00	0.00	0.00	0.00
Muscle	0.04	0.02	0.01	0.00	0.00	0.00	0.00	0.00	0.00	0.00
Bone	0.04	0.01	0.01	0.01	0.01	0.01	0.01	0.01	0.01	0.01
Salivary gland	0.19	0.03	0.03	0.00	0.01	0.00	0.01	0.00	0.00	0.00
Brain	0.01	0.00	0.00	0.00	0.01	0.00	0.00	0.00	0.00	0.00
Tail	0.40	0.08	0.09	0.07	0.05	0.04	0.04	0.04	0.05	0.05

Table S2. Biodistribution of ^{177}Lu-PSMA I&T at 1, 12, 24, 48 and 168 h after intravenous administration. Mean and SD of %ID/g and %ID are shown (n=5).

%ID/g	1 h		12 h		24 h		48 h		168 h	
	Mean	SD	Mean	SD	Mean	SD	Mean	SD	Mean	SD
Blood	3.05	3.77	0.06	0.01	0.02	0.01	0.01	0.01	0.00	0.00
Heart	0.66	0.32	0.17	0.04	0.08	0.03	0.03	0.03	0.00	0.00
Lung	0.81	0.52	0.29	0.05	0.14	0.05	0.07	0.03	0.03	0.01
Liver	0.32	0.19	0.08	0.02	0.04	0.01	0.03	0.02	0.01	0.00
Spleen	26.05	19.00	6.27	1.26	4.02	0.74	1.48	1.52	0.13	0.05
Pancreas	2.64	3.48	0.17	0.06	0.06	0.04	0.02	0.02	0.00	0.00
Kidneys	165.50	20.46	171.61	14.99	76.84	22.70	18.45	20.07	0.52	0.34
Stomach	0.21	0.10	0.14	0.07	0.07	0.03	0.03	0.02	0.00	0.00
Small intestine	0.16	0.11	0.09	0.03	0.03	0.01	0.02	0.01	0.00	0.00
Large intestine	0.18	0.08	0.42	0.19	0.55	0.71	0.06	0.03	0.01	0.01
Bladder	4.12	2.98	1.73	1.27	6.41	6.55	0.65	0.84	0.04	0.04
Testicles	0.85	0.18	0.30	0.11	0.28	0.17	0.20	0.12	0.16	0.06
Fat	1.39	0.71	1.08	0.46	0.69	0.13	0.56	0.79	0.06	0.11
Muscle	0.81	0.61	0.07	0.02	0.04	0.02	0.01	0.01	0.00	0.00
Bone	0.32	0.17	0.10	0.04	0.05	0.02	0.02	0.01	0.00	0.01
Salivary gland	1.07	0.88	0.47	0.12	0.18	0.04	0.08	0.06	0.01	0.00
Brain	0.24	0.30	0.02	0.01	0.02	0.00	0.01	0.00	0.01	0.00
Tail	0.73	0.66	0.21	0.07	0.10	0.02	0.04	0.02	0.01	0.00
%ID	**1 h**		**12 h**		**24 h**		**48 h**		**168 h**	
	Mean	SD	Mean	SD	Mean	SD	Mean	SD	Mean	SD
Blood	1.34	1.66	0.03	0.00	0.01	0.00	0.00	0.00	0.00	0.00
Heart	0.07	0.03	0.02	0.01	0.01	0.00	0.00	0.00	0.00	0.00
Lung	0.12	0.08	0.05	0.01	0.03	0.01	0.01	0.00	0.00	0.00
Liver	0.26	0.15	0.08	0.02	0.03	0.01	0.03	0.01	0.01	0.00
Spleen	0.73	0.54	0.19	0.04	0.07	0.01	0.02	0.02	0.00	0.00
Pancreas	0.38	0.47	0.02	0.01	0.01	0.01	0.00	0.00	0.00	0.00
Kidneys	53.37	1.11	52.95	4.12	23.51	6.53	5.22	5.54	0.14	0.08
Stomach	0.09	0.01	0.06	0.05	0.02	0.01	0.01	0.01	0.00	0.00
Small intestine	0.17	0.09	0.09	0.04	0.04	0.00	0.02	0.01	0.01	0.00
Large intestine	0.15	0.06	0.36	0.15	0.42	0.54	0.05	0.03	0.01	0.01
Bladder	0.09	0.09	0.03	0.02	0.13	0.16	0.01	0.01	0.00	0.00
Testicles	0.11	0.03	0.05	0.02	0.04	0.02	0.04	0.03	0.03	0.01
Fat	0.13	0.08	0.11	0.06	0.07	0.04	0.04	0.05	0.00	0.01
Muscle	0.09	0.07	0.01	0.00	0.00	0.00	0.00	0.00	0.00	0.00
Bone	0.02	0.01	0.01	0.00	0.00	0.00	0.00	0.00	0.00	0.00
Salivary gland	0.14	0.12	0.06	0.01	0.02	0.01	0.01	0.01	0.00	0.00
Brain	0.08	0.10	0.01	0.00	0.01	0.00	0.00	0.00	0.00	0.00
Tail	0.30	0.28	0.09	0.03	0.04	0.01	0.02	0.01	0.01	0.00

Table S3. Activity uptake in %ID/g of $^{19}F/^{177}Lu$-rhPSMA-7.3 and ^{177}Lu-PSMA I&T in LNCaP tumors and kidneys over 1 h to 168 h. Tumor-to-kidney ratios (T/K ratio) of $^{19}F/^{177}Lu$-rhPSMA-7.3 and ^{177}Lu-PSMA I&T from 1 h to 168 h were calculated by %ID/g values. Data are given as mean ± SD (n=5).

	1 h		12 h		24 h		48 h		168 h	
	rhPSMA	**PSMA I&T**	**rhPSMA**	**PSMA I&T**	**rhPSMA**	**PSMA I&T**	**rhPSMA**	**PSMA I&T**	**rhPSMA**	**PSMA I&T**
Tumor	12.4±1.4	4.4±1.5	11.4±2.2	5.5±1.7	9.9±3.1	6.2±1.9	9.5±3.2	4.3±2.4	4.5±1.8	1.0±0.2
Kidneys	207.6±31.0	165.5±20.5	164.3±29.6	171.6±15.0	28.7±16.5	76.8±22.7	14.4±11.0	18.5±20.1	0.5±0.1	0.5±0.3
T/K ratio	0.06±0.01	0.03±0.01	0.07±0.02	0.03±0.01	0.5±0.3	0.10±0.04	0.9±0.4	0.4±0.3	9.2±2.8	2.4±1.2

Table S4. Radiation doses (1 h voiding interval) for $^{19}F/^{177}Lu$-rhPSMA-7.3 calculated for the major organs and tissues of humans (adult male) using the OLINDA software.

Target Organ	Alpha	Beta	Photon	Total
Adrenals	0.00E+00	3.34E-04	3.16E-03	3.49E-03
Brain	0.00E+00	3.34E-04	2.88E-05	3.63E-04
Gallbladder wall	0.00E+00	3.34E-04	1.91E-03	2.24E-03
LLI wall	0.00E+00	3.34E-04	5.42E-04	8.76E-04
Small intestine	0.00E+00	3.34E-04	1.03E-03	1.36E-03
Stomach wall	0.00E+00	3.34E-04	1.22E-03	1.55E-03
ULI wall	0.00E+00	3.34E-04	1.02E-03	1.35E-03
Heart wall	0.00E+00	2.96E-03	5.01E-04	3.46E-03
Kidneys	0.00E+00	1.14E+00	2.04E-02	1.16E+00
Liver	0.00E+00	1.42E-02	1.82E-03	1.60E-02
Lungs	0.00E+00	4.24E-03	4.36E-04	4.68E-03
Muscle	0.00E+00	3.34E-04	5.28E-04	8.62E-04
Pancreas	0.00E+00	3.34E-04	2.35E-03	2.68E-03
Red marrow	0.00E+00	2.47E-04	7.98E-04	1.05E-03
Osteogenic cells	0.00E+00	1.07E-03	7.50E-04	1.82E-03
Skin	0.00E+00	3.34E-04	2.16E-04	5.50E-04
Spleen	0.00E+00	7.14E-02	4.13E-03	7.56E-02
Testes	0.00E+00	3.34E-04	2.23E-04	5.57E-04
Thymus	0.00E+00	3.34E-04	1.51E-04	4.85E-04
Thyroid	0.00E+00	3.34E-04	5.80E-05	3.92E-04
Urinary bladder wall	0.00E+00	9.51E-02	2.64E-03	9.77E-02
Total body	0.00E+00	5.62E-03	6.42E-04	6.26E-03

Table S5. Radiation doses (1h voiding interval) for ^{177}Lu-PSMA I&T calculated for the major organs and tissues of humans (adult male) using the OLINDA software.

Target Organ	Alpha	Beta	Photon	Total
Adrenals	0.00E+00	1.11E-03	3.49E-03	4.60E-03
Brain	0.00E+00	1.11E-03	9.19E-05	1.21E-03
Gallbladder wall	0.00E+00	1.11E-03	1.94E-03	3.06E-03
LLI wall	0.00E+00	1.11E-03	6.59E-04	1.77E-03
Small intestine	0.00E+00	1.11E-03	1.19E-03	2.31E-03
Stomach wall	0.00E+00	1.11E-03	1.40E-03	2.52E-03
ULI wall	0.00E+00	1.11E-03	1.17E-03	2.28E-03
Heart wall	0.00E+00	2.39E-03	5.39E-04	2.93E-03
Kidneys	0.00E+00	1.27E+00	2.29E-02	1.30E+00
Liver	0.00E+00	1.73E-03	1.49E-03	3.22E-03
Lungs	0.00E+00	4.24E-03	4.76E-04	4.72E-03
Muscle	0.00E+00	1.11E-03	6.23E-04	1.74E-03
Pancreas	0.00E+00	1.11E-03	2.61E-03	3.73E-03
Red marrow	0.00E+00	8.24E-04	9.34E-04	1.76E-03
Osteogenic cells	0.00E+00	3.58E-03	9.33E-04	4.51E-03
Skin	0.00E+00	1.11E-03	2.67E-04	1.38E-03
Spleen	0.00E+00	8.67E-02	4.81E-03	9.16E-02
Testes	0.00E+00	1.11E-03	2.90E-04	1.40E-03
Thymus	0.00E+00	1.11E-03	2.16E-04	1.33E-03
Thyroid	0.00E+00	1.11E-03	1.36E-04	1.25E-03
Urinary bladder wall	0.00E+00	9.44E-02	2.69E-03	9.71E-02
Total body	0.00E+00	6.67E-03	7.41E-04	7.41E-03

Table S6. Radiation doses in mGy/MBq for $^{19}F/^{177}Lu$-rhPSMA-7.3 and ^{177}Lu-PSMA I&T to LNCaP tumors calculated for different volumes (mL) using the OLINDA software.

Sphere/ Tumor volume (mL)	$^{19}F/^{177}Lu$-rhPSMA-7.3	^{177}Lu-PSMA I&T
0.01	9.26E+04	3.53E+04
0.1	9.64E+03	3.68E+03
0.5	1.96E+03	7.47E+02
1	9.90E+02	3.77E+02
2	4.97E+02	1.90E+02
4	2.49E+02	9.51E+01
6	1.67E+02	6.35E+01
8	1.25E+02	4.76E+01
10	1.00E+02	3.82E+01
20	5.01E+01	1.91E+01
40	2.52E+01	9.62E+00
60	1.69E+01	6.43E+00
80	1.27E+01	4.83E+00
100	1.02E+01	3.87E+00
300	3.42E+00	1.30E+00
400	2.57E+00	9.80E-01
500	2.06E+00	7.86E-01
600	1.72E+00	6.56E-01
1000	1.04E+00	3.97E-01
2000	5.27E-01	2.01E-01
3000	3.53E-01	1.35E-01
4000	2.66E-01	1.02E-01
5000	2.14E-01	8.16E-02
6000	1.79E-01	6.82E-02

Table S7. Tumor growth changes of the respective treatment and control groups in the endoradiotherapy study at days before/after treatment (day 0). Absolute volumes in mm^3 and relative tumor volumes as fold-change are given as mean ± SEM.

Time point (day prior/post treatment)	**Treatment group $^{19}F/^{177}Lu$-rhPSMA-7.3**		**Control group rhPSMA-7.3**	
	Tumor volume (mm^3)	Tumor volume (fold-change)	Tumor volume (mm^3)	Tumor volume (fold-change)
-5	147.5±7.3	1.0±0.0	122.8±38.2	1.0±0.0
1	222.6±18.8	1.5±0.1	190.8±38.6	1.8±0.2
8	157.7±23.1	1.1±0.1	480.0±92.0	4.5±0.6
14	118.2±17.6	0.8±0.1	599.1±246.1	5.2±0.8
23	126.6±18.2	0.9±0.1	771.0±95.1	12.7±2.0
30	106.5±15.5	0.7±0.1		
37	127.8±29.7	0.9±0.2		
42	170.3±46.1	1.2±0.3		
Time point (day prior/post treatment)	**Treatment group ^{177}Lu-PSMA I&T**		**Control group PSMA I&T**	
	Tumor volume (mm^3)	Tumor volume (fold-change)	Tumor volume (mm^3)	Tumor volume (fold-change)
-5	195.0±41.4	1.0±0.0	275.8±113.6	1.0±0.0
2	457.9±108.1	2.4±0.2	516.8±185.6	2.3±0.3
8	376.4±83.3	2.0±0.2	571.0±262.4	3.2±0.2
14	387.5±60.4	2.3±0.5	574.7±239.3	6.5±1.7
21	674.0±206.7	3.6±0.9	540.2±265.1	11.5±2.0
28	691.7±183.9	4.8±1.6	809.3	39.6
35	409.0±24.5	3.3±0.8		
43	712.2±119.4	6.2±2.7		